Chapter 25

Heat Release from Wood Wall Assemblies Using Oxygen Consumption Method

Hao C. Tran and Robert E White

Forest Products Laboratory, U.S. Department of Agriculture Forest Service, One Gifford Pinchot Drive, Madison, WI 53705–2398

The concept of heat release rate is gaining acceptance in the evaluation of fire performance of materials and assemblies. However, this concept has not been incorporated into fire endurance testing such as the ASTM E-119 test method. Heat release rate of assemblies can be useful in determining the time at which the assemblies start to contribute to the controlled fire and the magnitude of heat contribution. Twelve wood wall assemblies were tested in an ASTM E–119 fire endurance furnace at the USDA Forest Service, Forest Products Laboratory. Heat release measurements using the oxygen consumption method were a part of this program. The data demonstrate the usefulness of the oxygen consumption calorimetric technique for calculating heat release rate. The tests reconfirmed previous work that showed heat release from assemblies protected with gypsum board is negligible during the first 30 min and is significantly less than that of unprotected assemblies for the duration of the test. With proper specifications for the fire endurance furnace, such as air supply and furnace pressure, the method can be incorporated into the ASTM E-119 test standard. Accuracy of the method is discussed.

The measurement of heat release rate using the oxygen consumption method has been developed and perfected for a number of applications. The major applications include heat release rate calorimeters, such as the Cone Calorimeter developed by the National Institute of Standards and Technology (NIST) (formerly the National Bureau of Standards) *(1),* furniture calorimeters *(2),* room fire tests *(3),* and the ASTM E-84 tunnel test *(4).* Because heat release rate of assemblies undergoing fire endurance testing are useful in assessing the overall fire performance of the assemblies, there has been some interest in incorporating this methodology into standard fire endurance tests such as the ASTM E-119 test method *(5).* The standard ASTM E-119 test method is used to evaluate the ability of an assembly to resist a severe fire exposure and maintain structural integrity for a specified period. Heat release measurements indicate the contribution of the assembly to the intensity of the fire.

At the USDA Forest Service, Forest Products Laboratory (FPL), Brenden and Chamberlain (6) examined the feasibility of measuring heat release rate from an ASTM E–119 furnace. Three methods of measuring heat release were considered: the substitution method, oxygen consumption method, and weight of material/heat of combustion method. The oxygen consumption method was shown to be the most advantageous way to measure heat release. However, data were limited to a few assemblies. Chamberlain

In: Nelson, Gordon L., ed. Fire and polymers: Hazards identification and prevention. ACS symposium series 425. Proceedings of 197th national meeting of the American Chemical Society; 1989 April 9-14; Dallas, TX. Washington, DC: American Chemical Society: 1990. Chapter 25.

and King *(7)* used the substitution method to evaluate similar assemblies at another test facility.

Available analytical methods for determining the fire resistance (or fire endurance) of wood members have been reviewed by White *(8).* A finite-element heat transfer model for wood-frame walls was developed by the University of California–Berkeley *(9)* with funding from the FPL.

As a follow-up to previous work, we measured heat release rate for a series of 12 wall assemblies of four different constructions, using an improved gas sample analysis system and computer data acquisition.

Background

The heat release rate (amount of heat released per unit time) measures the potential of a material to contribute to a fire and has been the subject of many studies. The combustible volatiles produced when wood undergoes thermal degradation are responsible for flaming combustion and heat release. Browne and Brenden *(10)* calculated the heat of combustion of the volatile pyrolysis products of untreated and fire-retardant-treated ponderosa pine wood using an oxygen bomb calorimeter. By determining the heat of combustion of whole wood and partially pyrolyzed wood (char residue). they found heat of combustion of the volatile pyrolysis products varied with the degree of volatilization (pyrolysis). In general. heats of combustion of the volatile products were less than that of the original wood. Heat of combustion of the residual char was higher than that of the original wood.

Because heat of combustion of the volatile product is not the same as that of whole wood. one cannot estimate heat release rate based on mass loss rate as can be done with "ideal" fuels such as gases. liquids. and some noncharring solid materials. Thus. measuring heat release rate rather than mass loss rate is appropriate for wood and charring materials. Several bench-scale calorimeters have been developed to measure heat release rate of materials *(1,11,12,13).*

Some early calorimeters use "thermal" methods based on principles of heat and mass balance *(12)* and temperature rise of a constant flow of air through the combustion chamber *(13).* These calorimeters suffer from many drawbacks associated with their design. Heat and mass balance requires numerous measurements to account for all heat and mass flows. In most cases. thermal lag and losses in the equipment occur. which are not easily calculated.

Because of the problems associated with thermal methods, a gas analysis method, namely the oxygen consumption method, was devised. The landmark work for this method was done by Huggett *(14).* He documented that the heat release per unit oxygen consumed is approximately the same for a wide range of organic materials. For example, cellulose and cotton have a net heat of combustion of 13.6 MJ/kg O_2 consumed. For maple wood, the value is 12.5 MJ/kg O_2. The average is 13.1 MJ/kg O_2 for most materials; the general variability is within 5 percent of the mean or better. Thus. the rate of heat release can be calculated with confidence when the rate of oxygen consumed is known. Huggett *(14)* also showed that for incomplete combustion. when part of the combustion products are carbon monoxide. aldehydes. or carboxylic acids. the heat of combustion per unit oxygen consumed is not much different from the average heat of combustion, if concentrations of these products are small. If the products are present in large amounts, proper corrections can be applied. The oxygen consumption method measures the chemical heat release rate, which is the sum of two major components: convective and radiative *(15).*

Brenden and Chamberlain *(6)* measured heat release rate from wall assemblies having fire-retardant-treated studs and gypsum board as interior finish in the FPL fire endurance furnace using three methods: (a) the substitution method. by which the amount of fuel required to maintain the ASTM E–119 time-temperature curve for a

noncombustible wall assembly is compared with that required for the assembly being tested (thus, two tests must be conducted, one with a noncombustible assembly and the other with the test assembly): (b) the oxygen consumption method, by which the rate of heat release is related to the rate of oxygen consumed by the combustion of pyrolysis products from the assembly; and (c) the weight of material/heat of combustion method, by which the heat of combustion of the material at the beginning of the test is compared to the residual heat of combustion of the material at the end of the test (this method does not provide rate data; instead, the total heat release is obtained). Evidently, the oxygen consumption method is more advantageous because rate of heat release is obtained with one single test. Because of some difficulties in the gas sampling system, Brenden and Chamberlain made a few assumptions for the data reduction of the oxygen consumption method.

Chamberlain and King *(7)* used the substitution method to measure heat release from assemblies similar to those used by Brenden and Chamberlain *(6).* Steel stud walls of similar construction were used as reference. The heat release from the wood wall assemblies made of fire-retardant-treated framing and protected with type-X gypsum board was low enough to be within experimental error. The oxygen consumption method was attempted but it was not successful because of the complex geometry of the stack at the test facility, making measurement of flow of exhaust gases difficult.

The ASTM E–119 furnace available at the FPL is amenable to the implementation of the oxygen consumption method because (a) a long vertical exhaust duct is above the furnace, which allows combustion products to flow through without losses, and (b) the ratio of length to effective diameter of the exhaust is large enough to allow complete mixing of the exhaust gases. With the availability of modern equipment to monitor fire gases, we were able to refine heat release rate measurements.

Experimental Methods

The FPL vertical wall furnace used in our study was described in some detail by Brenden and Chamberlain *(6).* This furnace is normally used to evaluate the fire endurance of wall assemblies. The basic guidelines for the furnace test method are given in the ASTM E–119 standard *(5).* The method was designed to evaluate the ability of a structure to withstand a standard fire exposure that simulates a fully developed fire. The furnace is gas fired, and its temperature is controlled to follow a standard time–temperature curve. A load may be applied to the assembly. The failure criterion can be taken as time at burnthrough, structural failure, or a specified temperature rise on the unexposed side of the wall—whichever comes first. The construction of the furnace is not specified in the ASTM E–119 standard.

Twelve wood-frame walls were tested as part of a fire endurance research project to develop and verify models to predict the fire endurance of wood wall assemblies. The assemblies consisted of three groups. A, B, and C, using different construction types (Table I). Eight tests (Groups A and C) were based on a 2^3 factorial design involving the type of interior finish (plywood or gypsum board), presence of a fiberglass insulation in the cavity, and two load levels, 11.500 and 22,400 lb (51 and 100 kN). The four tests of Group B were the same as the tests in Groups A and C, except no load was applied and no hardboard siding was used. The wall tests of Group B were added to obtain the third set of replicate temperature profile data. The walls of Group B also provided information on heat release rates for a longer test duration.

Calibration Test. Before the wall tests were carried out, a calibration test was conducted to evaluate burner performance and to check for agreement between fuel gas and heat release calculations. For this test, the furnace was closed with a masonry wall lined with a layer of ceramic blanket material. The ASTM E–119 time-temperature curve was followed for 60 min.

Table I. Construction and Load Conditions of Wall Assemblies

Test no.	Siding	Load (lb)	Load (kN)	Interior finish [a]	Insulation
A-1	Hardboard	22.400	100	Plywood	No
A-2					Yes
A-3				Gypsum	No
A-4					Yes
B-1	None	0	0	Plywood	No
B-2					Yes
B-3				Gypsum	No
B-4					Yes
C-1	Hardboard	11.500	51	Plywood	No
C-2					Yes
C-3				Gypsum	No
C-4					Yes

[a] Interior finish for tests 1 and 2 of each group was plywood: finish for tests 3 and 4 was gypsum board.

Wall Assembly Construction. Because the materials and the design of the assemblies were specified in English units of measurement (for example 2 by 4 lumber, 24 in. on center). dimensions are expressed in English units with SI equivalents. By contrast, our equipment is calibrated in SI units, and consequently SI units are used in the remaining sections of this paper.

The 8 by 10 ft (2.44 by 3.05 m) walls for fire endurance tests were constructed of nominal 2 by 4 in. (38 by 89 mm) Douglas-fir or larch wood studs 24 in. (0.61 m) on center. The moisture contents of the studs ranged from 8.1 to 13.2 percent and their densities from 430 to 710 kg/m^3. The exterior sheathing was 5/8-in.- (16-mm-) thick C–D plywood with exterior glue. A double nominal 2 by 4 in. (38 by 89 mm) plate was at the top and a single plate was at the bottom. The plywood interior finish was 5/32-in.- (4-mm-) thick, simulated wood grain finish plywood paneling. The gypsum board interior finish was 5/8-in.- (16-mm-) thick, type-); (fire-rated) gypsum board. The insulation was 3.5-in.- (90-mm-) thick, unfaced, glass-fiber insulation (friction-fit). Walls with insulation also had a 4-mil clear polyethylene vapor barrier on their interior side. All wood and gypsum materials were conditioned at 23°C and 50 percent relative humidity, resulting in moisture content of 9 to 10 percent in wood materials. Figure 1 is a diagram of the wall frame construction. The hardboard siding was on the exterior side of the 5/8-in. (16-mm) plywood (not shown).

Furnace Operating Conditions. The furnace pressure was normally slightly positive at the top and negative at the bottom. In an effort to increase air supply. an additional blower was added for runs B–2. B–3. and B–4. We found no significant increase in air flow out of the stack. However. the furnace pressure increased significantly. resulting in significant leaks into the testing environment. Thus, we decided to use the original air supply system. To increase air available for complete combustion of pyrolysis products from the wall, the gas burners were adjusted to have a wider range. The lower limit was changed from 500 kW to 250 kW in series B and C. This helped provide more air to oxidize wood materials. especially when wood contribution was greatest. The operating conditions are summarized in Table II.

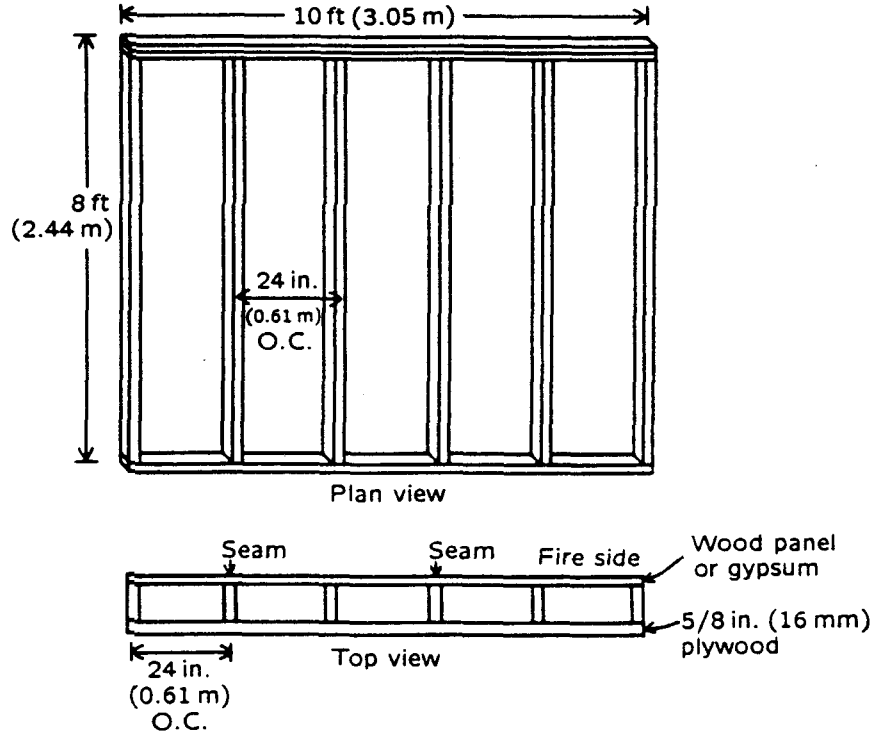

Figure 1. Construction details for wall assemblies (not to scale).

Table II. Furnace Operating Conditions

Test no.	Burners (kW)	Pressure		Approximate test termination time [a] (min)
		Bottom	Top	
A–1	500–850	–	+	8
A–2		–	+	12
A–3		–	+	33
A–4		–	+	37
B–1	250–850	–	+	14
B–2		+	+	20
B–3		+	+	52
B–4		+	+	60
C-1	250–850	–	+	13
C–2		–	+	17
C–3		–	+	46
C–4		–	+	52

[a] For series A and C. these times correspond to structural failure. For series B. they correspond to burnthrough.

Instrumentation. To calculate rate of heat release on the basis of oxygen consumption. the flow rate of air into the system and the species concentrations in the stack must be measured. The furnace is operated by forced air via a blower. The amount of air coming into the system is split into two streams, called primary and secondary air. The pressure of the primary air is controlled to regulate the fuel-air mixture. The primary air pressure controls the amount of gas input to the burners. The secondary air is the bulk of the incoming air. which acts as a diluent to lower the temperature of the exhaust gases and supplies oxygen to the whole system. The incoming flow was not measured because of the complexity of the piping system; instead. flow rate out of the stack was continuously monitored.

We measured flow rate out of the system with a bidirectional probe placed at the center of the exhaust stack, which has a rectangular cross section of 12 by 20 in. (0.3 by 0.5 m). The equivalent diameter of the exhaust stack is 15 in. (0.38 m). The probe was positioned near the top of the 12-ft- (3.66-m-) long stack. The ratio of length to diameter of the duct (L/D) was close to 10:1. This distance ensured that the stack gas was well mixed prior to sampling. Two thermocouples were placed in the same cross section of the duct, one attached to the bidirectional probe and the other between the probe and the wall of the stack. A sample of the exhaust gases was pumped to the sampling system. The tube between the sample probe and the sampling system was heat traced to prevent water condensation. The location of the bidirectional probe. thermocouple. and gas sample probe in the duct is shown in Figure 2.

The sample handling system is diagrammed in Figure 3. As shown. the concentrations of oxygen. carbon monoxide. and carbon dioxide were on a dry basis because the water was removed. The water vapor analyzer did not function properly because condensation occurred in the instrument when water vapor was too high. often exceeding 20 percent. By using some approximations in the calculations. we did not need the exact concentration of water.

The flow rate of fuel gas into the furnace was measured using a volumetric flow meter. Data were collected every 30 s using a personal computer.

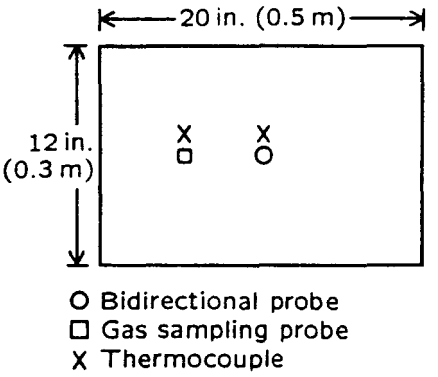

Figure 2. Location of probes and thermocouples in stack (cross section).

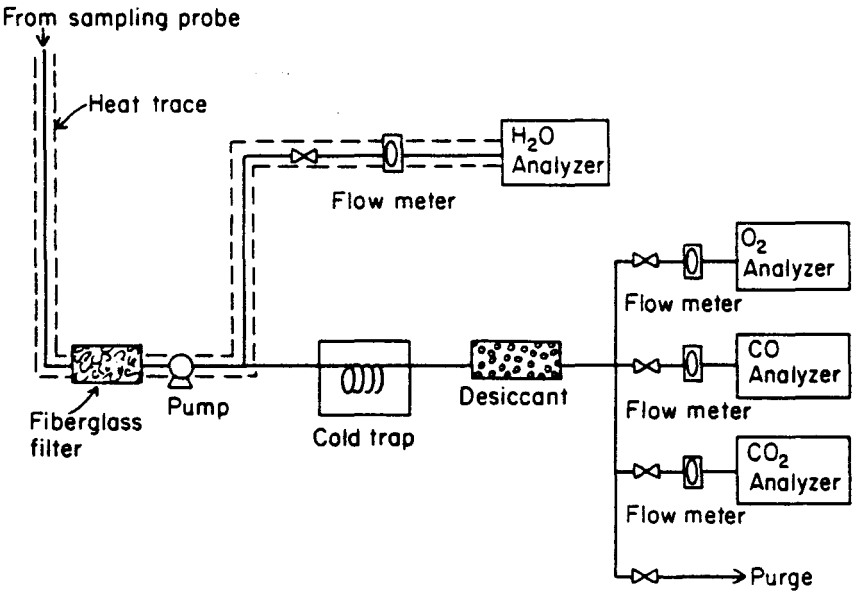

Figure 3. Sampling handling system for gas analysis.

Data Reduction and Calculations

Calculations of heat release rate by the oxygen consumption method as described by Parker *(16)* for various applications will be used here. Basically, heat release by the wall is heat release rate as measured in the furnace stack using the oxygen consumption method minus the heat release rate from the fuel gas. The comprehensive equation for heat release rate of the materials ($\dot{Q}_{wall}$) as given in Parker's paper *(16)* is

$$\dot{Q}_{wall} = \left[1 - \frac{X_{O_2}}{X^0_{O_2}}\left(\frac{1 - X^0_{O_2} - X^0_{CO_2}}{1 - X_{O_2} - X_{CO} - X_{CO_2}}\right)\left(1 + \frac{E'_{CO} - E'}{2E'}\frac{X_{CO}}{X_{O_2}}\right)\right] E' X^0_{O_2} \dot{V}_0 - E' r' \dot{V}_g \quad (1)$$

where

$X_{O_2}, X_{CO}, X_{CO_2}$ are volume (or molar) fractions of gas species as obtained in analyzers.

$X^0_{O_2}, X^0_{CO_2}$ are ambient concentrations of gas species (assuming concentrations of O_2 and CO_2 of 21 percent and zero, respectively).

E' is heat release per volume of oxygen consumed. 17.2 MJ/m³ at 25°C or 17.4 MJ/m³ at 20°C (values based on average of 13.1 MJ/kg of oxygen consumed).

E'_{CO} heat produced per unit volume of oxygen consumed in burning of CO to CO_2. 23.1 MJ/m³ O_2 at 25°C or 23.1 MJ/m³ at 20°C.

$\dot{V}_0$ volume flow rate of air into system, corrected to a standard temperature (20°C).

r' volume of O_2 consumed in burning a unit volume of fuel. and

$\dot{V}_g$ volume flow rate of gas into the furnace. corrected to 20°C.

We used volumetric flows of air and fuel gas because they were directly measured. Using volumetric flow rates is awkward because the temperature and pressure of the gases in question have to be specified. In our case. the pressure of the fuel gas supply was about 1.5 kPa and that of the furnace 25 Pa above atmospheric pressure in extreme cases. These gauge pressures are small compared to absolute atmospheric pressure of >100 kPa. Thus, pressure corrections are insignificant. Temperature is the main factor that needs to be specified as the reference or basis for volumetric flow calculation. One alternative is the substitution of volumetric flow by mass flow. The conversion from volumetric flow to mass flow is straightforward using proper density values of the gases in question. The average heat of combustion of 13.1 MJ/kg of O_2 consumed is then applicable. However, for the purposes of this paper. either method will yield the same result.

Heat Release Rate From Furnace. Heat release rate from the furnace ($\dot{Q}_{furnace}$) is calculated from the information obtained in the stack: flow rate and species concentrations. Heat release rate is based on the first term in Equation 1.

$$\dot{Q}_{furnace} = \left[1 - \frac{X_{O_2}}{X^0_{O_2}}\left(\frac{1 - X^0_{O_2} - X^0_{CO_2}}{1 - X_{O_2} - X_{CO} - X_{CO_2}}\right)\left(1 + \frac{E_{CO} - E'}{2E'}\frac{X_{CO}}{X_{O_2}}\right)\right] E' X^0_{O_2} \dot{V}_0 \quad (2)$$

When there is complete combustion, X_{CO} is negligible. Equation 2 is simplified to

$$\dot{Q}_{\text{furnace}} = \left[1 - \frac{X_{O_2}}{X^0_{O_2}}\left(\frac{1 - X^0_{O_2} - X^0_{CO_2}}{1 - X_{O_2} - X_{CO_2}}\right)\right] E' X^0_{O_2} \dot{V}_0 \tag{3}$$

In our tests, the furnace was occasionally deficient of oxygen. When oxygen level went to zero, a significant amount of CO was produced as well as visible and sooty smoke. These are indications of incomplete combustion. The only product of incomplete combustion monitored was CO. Incomplete combustion products other than CO were not accounted for.

When X_{O_2} approaches zero, the term in the square brackets of Equation 2 approaches 1 or results in errors in the data reduction program because of X_{O_2} in the numerator and/or denominator. Equation 2 needs some modification to be sensitive to CO in these cases.

When $X_{O_2} \rightarrow 0$ and $(X_{CO}/X_{O_2}) >> 1$, Equation 2 can be approximated by

$$\dot{Q}_{\text{furnace}} = \left[1 - \frac{X_{O_2}}{X^0_{O_2}}\left(\frac{1 - X^0_{O_2} - X^0_{CO_2}}{1 - X_{CO} - X_{CO_2}}\right)\left(\frac{E'_{CO} - E'}{2E'}\frac{X_{CO}}{X_{O_2}}\right)\right] E' X^0_{O_2} \dot{V}_0 \tag{4}$$

which can be rearranged to

$$\dot{Q}_{\text{furnace}} = \left[1 - \frac{X_{CO}}{X^0_{O_2}}\left(\frac{1 - X^0_{O_2} - X^0_{CO_2}}{1 - X_{CO} - X_{CO_2}}\right)\left(\frac{E'_{CO} - E'}{2E'}\right)\right] E' X^0_{O_2} \dot{V}_0 \tag{5}$$

Air Flow Rate Into System. The flow rate into the system is calculated based on the flow rate out of the system and an assumed expansion factor (α). The flow rate of exhaust air coming out of the system corrected to 20°C ($\dot{V}_s$) is based on the differential pressure across the bidirectional probe and the average temperature in the stack:

$$\dot{V}_s = 0.926 k A \left(\frac{2\Delta P}{\rho_0}\frac{T_0}{T}\right)^{1/2} \tag{6}$$

where

- 0.926 is a suitable calibration factor for bidirectional probe,
- k the calibration factor for velocity profile in the stack (found to be 0.55 by Brenden and Chamberlain *(6))*,
- ΔP differential pressure in pascals,
- A cross-sectional area of stack, 0.155 m^2,
- T_0 reference temperature, 293 K,
- ρ_0 density of air at reference temperature, and
- T average temperature in stack in kelvins.

The chemical expansion a is defined as

$$\alpha = 1 + X^0_{O_2}(\beta - 1) \tag{7}$$

where ß is the ratio of the moles of combustion products formed per mole of oxygen consumed. Parker *(16)* documented that for most materials, a ranges from 1.00 for carbon to 1.21 for hydrogen, with most organic fuels about 1.1. We assumed a = 1.084 as recommended for most fuels in another application (3). A more accurate assumption can be made if the stoichiometry of combustion is known.

The flow rate into the system is related to the flow rate out as follows:

$$\dot{V}_s = (1 - \phi)\dot{V}_0 + \alpha\phi\dot{V}_0 \tag{8}$$

rearranged to give

$$\dot{V}_0 = \frac{\dot{V}_s}{1 + (\alpha - 1)\phi} \tag{9}$$

where ϕ is the depletion fraction, the fraction of the incoming air that has been totally depleted of its oxygen, which can be calculated based on the oxygen to nitrogen ratios in the incoming air and the stack (16) as

$$\phi = 1 - \frac{Z}{Z_0} \tag{10}$$

where Z and Z_0 are oxygen to nitrogen ratios in the stack and ambient air. respectively.

Equation 10 can be expanded to

$$\phi = 1 - \frac{(X_{O_2}/X^0_{O_2} - X_{O_2})}{(1 - X_{O_2} - X_{CO} - X_{CO_2})} \tag{11}$$

This equation allows us to calculate ϕ based on the species fractions.

Heat Release Rate From Fuel Gas. The fuel gas used in these tests was a mixture of natural gas supplied by the local gas company. This gas mixture contains approximately 90 percent methane and small fractions of ethane. propane. butane. CO_2, and nitrogen, as analyzed by Brenden and Chamberlain *(6).* Although composition of the gas changes with time. the changes were small in our case. A statistical sample of gross heat of combustion of fuel gas over several months showed a coefficient of variation of 0.7 percent. Also. the gross heat of combustion of natural gas reported by the gas company on the day of the test did not vary significantly from test to test. Thus. we assumed that the net heat of combustion was constant.

Net heat of combustion was calculated based on the gross heat of combustion and the stoichiometry of combustion of the fuel mixture and a typical composition of the fuel mixture. The rate of heat release from burning fuel gas ($\dot{Q}_{fuel}$) is

$$\dot{Q}_{fuel} = \Delta H_g \dot{V}_g \tag{12}$$

where

ΔH_g is net heat of combustion of fuel gas, 33.9 MJ/m^3 at 20°C, and

$\dot{V}_g$ volumetric flow rate of fuel gas in cubic meters per second at 20°C.

Heat Release Rate From Walls. The heat release rate from the wall assemblies should be the difference between $\dot{Q}_{furnace}$ and $\dot{Q}_{fuel}$. However. a direct subtraction is not correct because of the assumption that 13.1 MJ/kg oxygen consumed is released for all fuels. In fact. the heat release per unit oxygen consumed is 12.54 MJ/kg for methane as given by Huggett *(14)* and 12.51 MJ/kg for the fuel mixture as determined by Brenden and Chamberlain *(6).* Thus, the heat release from the wall $\dot{Q}_{wall}$ is determined using a correction factor of 13.1/12.51 = 1.048:

$$\dot{Q}_{wall} = \dot{Q}_{furnace} - 1.048\dot{Q}_{fuel} \tag{13}$$

The term $1.048\dot{Q}_{fuel}$ is essentially the same as the second term in Equation 1 because $E'r' = (E'/E'_g)\Delta H_g$, where E'_g is the correct E' value for fuel gas.

Results and Discussion

Heat release rates from the calibration run and the walls were made using Equations 1 to 13. The fire endurance results will be discussed in another paper. The tests were terminated shortly after structural failure or burnthrough of the wall assembly. The test termination times are given in Table II.

Calibration Test. Heat release rate is shown in Figure 4. Note that the heat release rate of the fuel calculated based on Equation 6 is slightly less than that of the total heat release. The heat release from the noncombustible wall calculated by Equation 13, using the proper correction of 1.048, is zero. Except for some perturbations in the beginning, which can be attributable to approximated response times of the analyzers, there is excellent agreement between the heat input by burning fuel gas and the total heat release rate calculated. We encountered a problem synchronizing the heat release rate calculated and the fuel gas rate because of the discrete data sampling time. The imperfectly synchronized rates resulted in "noises" in their differences, especially at the beginning of the test. No effort was made to interpolate data to match the two rate curves.

Heat Release Rate of Wall Assemblies. As examples, heat release rates are shown for series B because these tests lasted for longer times than the tests in series A and C (Figures 5–8). In walls B–3 and B–4, which had gypsum as the interior finish, combustion was complete throughout the entire runs. The concentration of CO was negligible.

In many cases when combustion was incomplete because of lack of oxygen, a significant amount of CO was formed. This amount of CO may further combust to CO_2 if extra air is added. Therefore. we can estimate the additional energy to be released if CO was allowed to burn to CO_2. The flow rate of CO can be calculated as follows:

$$\dot{V}_{CO} = X_{CO}\dot{V}_0\frac{X^0_{N_2}}{X_{N_2}} \tag{14}$$

where the concentration of N_2 is on a dry basis. Equation 14 is expanded to

$$\dot{V}_{CO} = 0.79\dot{V}_0\frac{X_{CO}}{(1 - X_{O_2} - X_{CO} - X_{CO_2})} \tag{15}$$

The flow rate of CO is multiplied by the heat of combustion of CO (11.7 MJ/m^3 of CO at 20°C) to obtain the heat release rate from CO if CO burns to CO_2. This heat release rate plus heat release rate from the wall is the potential heat release rate if CO is further oxidized to CO_2.

For walls B–1 and B–2, which had plywood as the interior finish. the heat release rate from the furnace (burners plus wall), heat release rate from the wall, and potential heat release rate are shown in Figures 5 and 6. The difference between the potential heat release rate and the wall contribution is the possible contribution by CO.

For those walls protected by gypsum (walls B–3 and B–4), furnace heat release rate and heat release rates from the fuel gas (Eq. (12)) and the wall (Eq. (13)) are shown in Figures 7 and 8. Similar to the noncombustible wall, the gypsum provided very little heat. except for a small peak in the beginning, which could have been caused by the gypsum paper. Heat release rates from walls B–3 and B–4 rose slowly as a result of the gypsum opening up at the seams or cracks.

Total Heat Release From Wall Assemblies. We examined the total heat release from the wall assemblies as total heat contribution. The total heat release is obtained by integrating the area under the heat release rate curve with time and it is expressed in megajoules (MJ). The total heat release data from ignition to different times are shown in Table III for the wall assemblies.

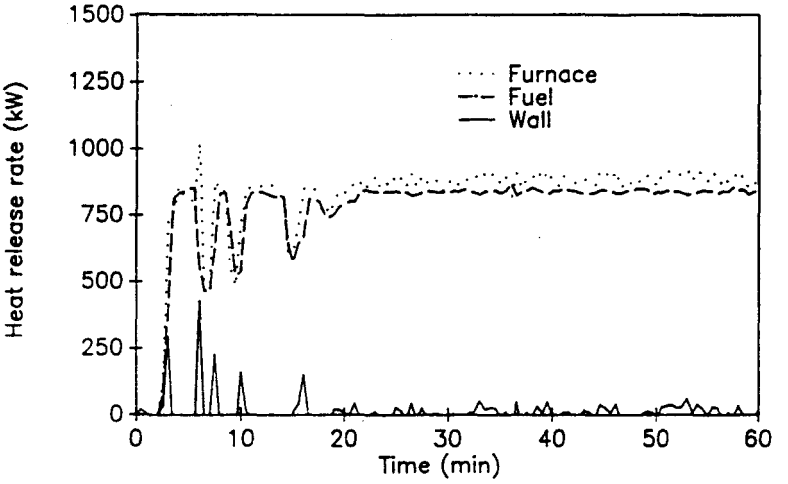

Figure 4. Heat release rate from calibration test with a blank wall.

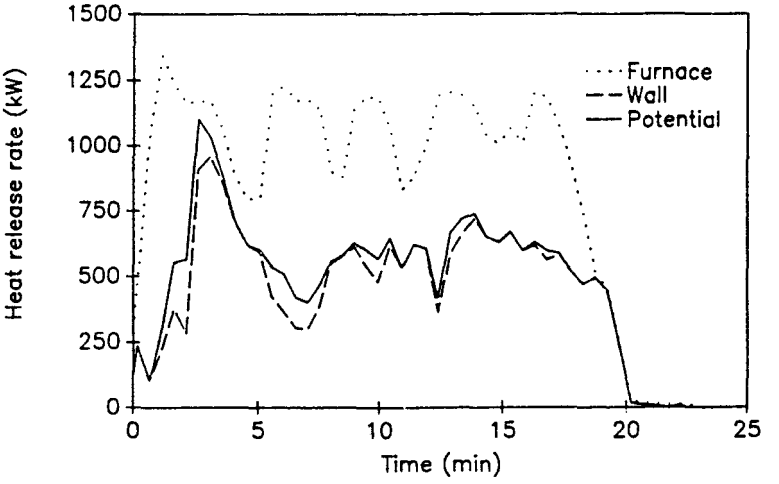

Figure 5. Rate of heat release for wall test B–1.

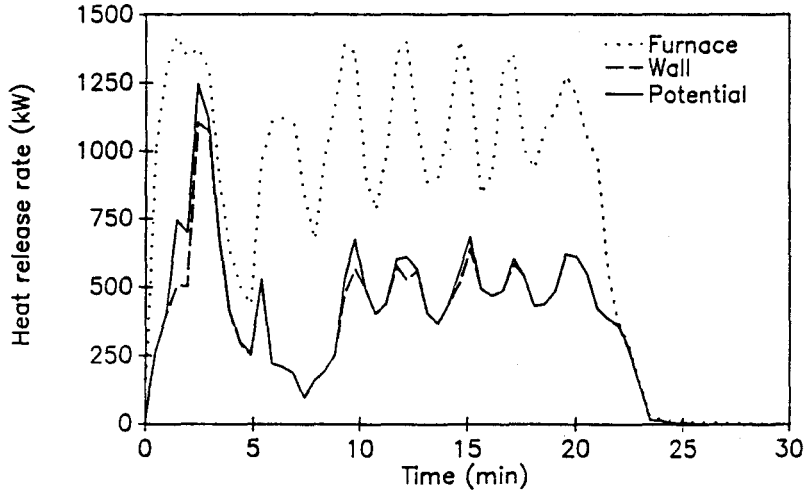

Figure 6. Rate of heat release for wall test B–2.

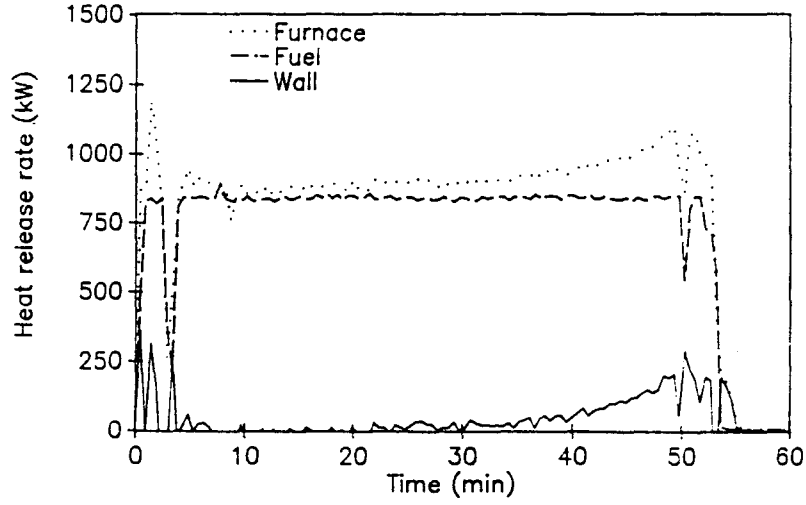

Figure 7. Rate of heat release for wall test B–3.

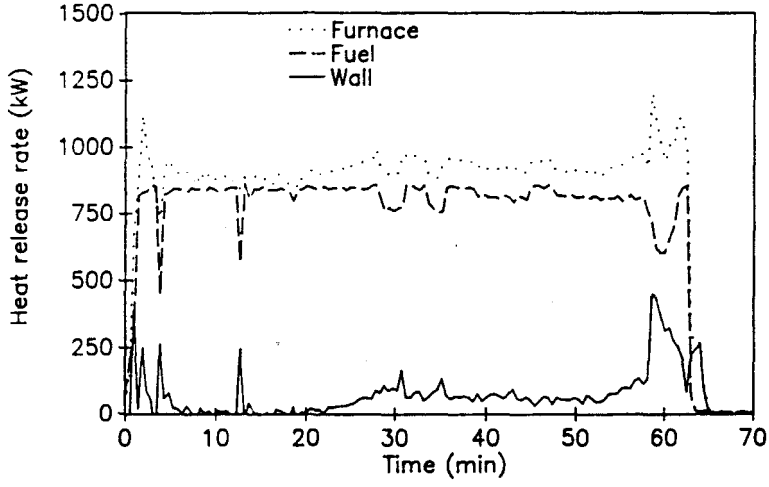

Figure 8. Rate of heat release for wall test B-4.

Table III. Total Heat Release From the Wall Assemblies

	Total Heat Release (MJ)							
Test no.	5 min	10 min	15 min	20 min	25 min	30 min	35 min	40 min
A–1	120	285	342	—	—	—	—	—
A–2	140	183	299	—	—	—	—	—
A–3	34	36	31	28	25	27	39	52
A–4	–11	–10	–16	–22	–27	–15	–5	17
B–1	196	350	533	687	—	—	—	—
B–2	181	280	434	586	650	—	—	—
B–3	28	23	20	20	21	28	36	49
B–4	30	33	40	40	48	70	96	117
C-1	200	390	517	518	—	—	—	—
C–2	195	265	424	588	—	—	—	—
C–3	29	38	41	48	59	72	89	117
C–4	40	51	56	61	77	94	115	138

In general, walls A–1, B–1, and C–1 had the highest heat release. Walls A–2, B–2, and C–2 had consistently less heat contribution because of the insulation. Walls A–3, B–3, and C–3 and A–4, B–4, and C–4 had no significant heat contribution. The values in these tests vary because of initial errors associated with the perturbations at the beginning of the tests. However, total heat release did not grow, indicating zero heat release rate when gypsum was present.

As we have noted, eight tests (series A and C) represented a 2^3 factorial design involving type of interior finish, presence of a fiberglass insulation in the cavity, and load level (Table I). Series B was similar to A and C except for the absence of load and hardboard siding. In most cases, the four tests of series B could also be included in the analysis.

The factorial approach to the design of experiments allows all the tests involving several factors to be combined in the calculation of the main effects and their interactions. For a 2^3 design, there are 3 main effects. 3 two-factor interactions, and 1 three-factor interaction. Yates' algorithm can be used to determine the main effects and their interactions *(17).* The data can also be represented as a multiple linear regression model

$$y = B_0 + B_1x_1 + B_2x_2 + B_3x_3 + B_4x_1x_2 + B_5x_1x_3 + B_6x_2x_3 + B_7x_1x_2x_3 \qquad (16)$$

where y is the response variable, r_i is the factor variable for factor i, and B_j are parameters.

By eliminating insignificant variables, Equation 16 can be reduced to fewer terms. In addition to the three variables of the factorial design, the burner level was also included in the analysis.

Because of the large difference in the behavior of the thin plywood and the gypsum board, the type of interior finish was the dominant factor in the statistical analysis of the total heat release data (Table 111). Linear regression of the data sets for 5, 10, and 15 min resulted in squares of the correlation coefficients R^2 = 0.88 to 0.91 with the type of interior finish as the sole variable. For the plywood, the average total heat release was 172, 292, and 425 MJ at 5, 10, and 15 min, respectively. For the gypsum board, the average total heat release was 25, 27, and 29 MJ at 5, 10, and 15 min. respectively.

For 5 min. the type of burner (lower limit of 250 kW (series B and C) compared to 500 kW (series A)) also had a significant effect. For a linear regression model with interior finish and the burner level as the variables. the R^2 = 0.96. Because the burner level primarily affected the total heat release from the plywood. the cross-product of burner level and type of interior finish is also a significant factor. At 10 min, the presence of insulation was more significant than the burner level. For a model with interior finish. insulation, and burner level as variables. the R^2 = 0.95 for 10-min data. At 15 min. insulation was no longer a significant factor. This is consistent with the visual observations that the insulations in the plywood tests were gone after approximately 10 min. A model of interior finish and burner level had an R^2 = 0.96 for the 15-min data. At 20 min, only the type of interior finish was a significant main factor [the cross-product of interior finish and burner was also significant). By 20 min, nearly all the plywood tests had been terminated.

Except for the load level. which should not have an effect on the total heat release, series B and C were identical. Comparison of the results for 5, 10, and 15 min indicates very good agreement between the two sets of data.

Comparison of Study to Previous Work. The only work that can be compared to ours is that of Brenden and Chamberlair. *(6)* using the same furnace and Chamberlain and King *(7)* using a different furnace. The assemblies used in these studies were of similar construction. The wall assemblies used contained fire-retardant-treated studs as the only combustibles. The interior and exterior sides were 5/8-in. (16-mm) type-X gypsum. Thus. heat release rates were understandably small. The onset of heat release started at 23 min after ignition. After that. a slow increase occurred. culminating to approximately 100 Btu/min · ft^2 (19 kW/m^2) at 60 min. For an exposed area of 8 by 10 ft (2.44 by 3.05 mm), this would be 140 kW.

Our results are comparable to the results of Brenden and Chamberlain (6) and Chamberlain and King *(7).* In our most comparable assembly having gypsum on the fire-exposed side and no insulation (B–3) (Fig. 7). contribution from the walls started approximately at 30 min and rose to about 200 kW at 50 min. Similar results were obtained despite differences in assembly constructions. The exterior sheathing in our tests was plywood whereas that of Brenden and Chamberlain *(6)* was gypsum. Moreover, we used untreated wood studs in our assemblies.

Accuracy of Oxygen Consumption Method. We have demonstrated that the oxygen consumption method can be used to quantify the amount of heat contributed to the fire environment by the walls. The heat release rate can be used as a diagnostic tool to evaluate performance of assemblies in question.

However, many possible sources of error other than the accuracy of the measurements deserve attention. These sources of error are inherent in the assumptions that we made about average *E'.* chemical expansion factor. and effect of dilution.

Average E^v—As stated earlier, the oxygen consumption method is based on the finding that most materials have the same *E',* with accuracy within 5 percent of the mean.

Chemical expansion factor—The values of α and β vary from material to material as shown by Parker *(16).* The values of α vary from 1.00 for carbon to 1.21 for hydrogen. Thus. extreme errors in α can be 10 percent from the mean, especially when ϕ = 1.0. An erroneous α results in wrong estimates of air flow rate into the system. which may lead to a maximum of 10 percent error in heat release rate.

Effect of dilution—In addition to the water present in the ambient air, the materials contained a certain amount of water. The water evaporated from the materials "diluted" the exhaust gases. This water is not accounted for in the chemical expansion factor. The magnitude of the error depends on the evaporation rate of water and the total

flow rate out the exhaust stack. Because we did not have an accurate measurement of water vapor in the exhaust stream. the effect of dilution was not calculated. This error can be large at the start of the test when water is boiled out of the system and should become negligible thereafter.

Of all these sources for error. the first two are the most significant. The oxygen consumption method has been reported to be accurate within 15 percent, which is the additive effect of average E' and the chemical expansion factor. This extreme error can happen only in the case of complete oxygen depletion. The error is substantially reduced for most cases when the oxygen level in the exhaust is larger than zero. As shown in the calibration test. very good agreement between $\dot{Q}_{\text{furnace}}$ and $\dot{Q}_{\text{fuel}}$ was obtained. The method is accurate at least for fuel gas alone.

Conclusion

Several conclusions can be drawn from the analysis of heat release rate in this study. In terms of heat contribution from the walls, the gypsum wallboard provided complete protection to the assembly for 30 min. Even after 30 min, heat release rate from the assembly was below 200 kW up to 60 min of exposure compared to the 600 kW from the assemblies without gypsum. The insulation also helped protect the assemblies, although not as dramatically as gypsum; it reduced heat release rate between 5 and 10 min.

The versatility and accuracy of the oxygen consumption method in heat release measurement was demonstrated. The critical measurements include flow rates and species concentrations. Some assumptions need to be invoked about (a) heat release per unit oxygen consumed and (b) chemical expansion factor, when flow rate into the system is not known. Errors in these assumptions are acceptable. As shown. the oxygen consumption method can be applied successfully in a fire endurance test to obtain heat release rates. Heat release rates can be useful for evaluating the performance of assemblies and can provide measures of heat contribution by the assemblies. The implementation of the heat release rate measurement in fire endurance testing depends on the design of the furnace. If the furnace has a stack or duct system in which gas flow and species concentrations can be measured. the calorimetry method is feasible. The information obtained can be useful in understanding the fire environment in which assemblies are tested.

One critical factor that affects the heat release rate is the availability of air. The furnace has to be designed so that many requirements can be met simultaneously: (a) time-temperature curve of ASTM E–119. (b) adequate air supply. and (c) pressure requirement inside the furnace. To incorporate the heat release rate measurement into the ASTM E–119 standard. specifications must be made to address these three criteria. If these criteria can be agreed upon, the heat release rate measurement should be made a part of the existing test standard.

Literature Cited

1. Babrauskas, Vytenis, *Development of the Cone Calorimeter—A Bench-scale Heat Release Rate Apparatus Based on Oxygen Consumption.* U.S. Department of Commerce NBSIR 82–2611. 1982.
2. Babrauskas, Vytenis. *J. Fire Sci.* 1983. 1, 9–32.
3. ASTM Annual Book of Standards. Proposed method for room fire test of wall and ceiling materials and assemblies. American Society for Testing and Materials: Philadelphia. PA. 1983: Vol. 04.07, pp. 958–978.
4. Parker, William J. *An Investigation of the Fire Environment in the ASTM E–84 Tunnel Test.* NBS Tech. Note 945. National Bureau of Standards: Washington. DC, 1977.

5. ASTM Annual Book of Standards. Standard methods of building construction and materials. Method E 119–83. American Society for Testing and Materials: Philadelphia, PA, 1985.
6. Brenden, John J.; Chamberlain. David L. *Heat Release Rates From Wall Assemblies: Oxygen Consumption and Other Methods Compared.* Res. Pap. FPL–RP–476. U.S. Department of Agriculture, Forest Service. Forest Products Laboratory: Madison, WI, 1986.
7. Chamberlain, David L.; King. Edward G., Jr. *Heat Release Rates of Construction Assemblies by the Substitution Method.* National Forest Products Association. Technical Report No. 9, 1987.
8. White, Robert H. In *SFPE Handbook of Fire Protection Engineering.* National Fire Protection Association, 3–130–3–142:Quincy, MA, 1988; Chapter 8.
9. Gammon, Barry W. Ph.D. Thesis, University of California, Berkeley, 1987.
10. Browne, F.L.; Brenden, J.J. *Heat of Combustion of the Volatile Pyrolysis Products of Fire-retardant-treated Ponderosa Pine.* Res. Pap. FPL 19. U.S. Department of Agriculture, Forest Service, Forest Products Laboratory: Madison, WI, 1964.
11. Teaarson, Archibald. In *Flame Retardant Polymeric Materials;* Lewin, M., Atlas, S.M., and Pearch, E.M., Eds.; Plenum Press: New York, 1982: Vol. 3. Ch. 3.
12. Brenden. John J. *J. Fire Flammability,* 1975. *6,* 274–293.
13. ASTM Annual Book of Standards. Standard test method for heat and visible smoke release rates for materials and products. Test Method E 906–83. American Society for Testing and Materials: Philadelphia, PA. 1985.
11. Huggett, Clayton. Fire Materials 1980.4. 61–65.
15. Tewarson, Archibald. In The SFPE Handbook of Fire Protection Engineering. DiNenno, P.J.. Ed.; The National Fire Protection Association Press: Quincy. MA, 1988; Ch. 13, Sec. I.
16. Parker, William J. *J. Fire Sci.* 1981, *2.* 380–395.
17. Box, George E.P.; Hunter, William G.; Hunter, Stuart J. Statistics for Experimenters. John Wiley & Sons: New York, 1978.

RECEIVED November 1, 1989